Study of methane oxidation over alumina supported Pd–Pt catalysts using operando DRIFTS/MS and in situ XAS techniques

Natalia M. Martin, Johan Nilsson, Magnus Skoglundh, Emma C. Adams, Xueting Wang, Gudmund Smedler, Agnes Raj, David Thompsett, Giovanni Agostini, Stefan Carlson, Katarina Norén & Per-Anders Carlsson

Taylor & Francis
Taylor & Francis Group

ORIGINAL RESEARCH PAPER

⊘ OPEN ACCESS

Study of methane oxidation over alumina supported Pd–Pt catalysts using *operando* DRIFTS/MS and *in situ* XAS techniques

Natalia M. Martin[a] ⓘ, Johan Nilsson[a] ⓘ, Magnus Skoglundh ⓘ[a], Emma C. Adams[a] ⓘ, Xueting Wang[a], Gudmund Smedler[b], Agnes Raj[c], David Thompsett[c], Giovanni Agostini[d], Stefan Carlson[e], Katarina Norén[e] and Per-Anders Carlsson[a] ⓘ

[a]Competence Centre for Catalysis, Chalmers University of Technology, Gothenburgh, Sweden; [b]Johnson Matthey AB, Västra Frölunda, Sweden; [c]Johnson Matthey, Reading, UK; [d]European Synchrotron Radiation Facility, Grenoble, France; [e]MAX-IV Laboratory, Lund University, Lund, Sweden

ABSTRACT

Methane oxidation over Pd–Pt/Al_2O_3 model catalysts calcined at three different conditions is investigated using *operando* diffuse reflectance infrared Fourier transform spectroscopy and mass spectrometry, and *in situ* X-ray absorption spectroscopy while cycling the feed gas stoichiometry between lean (net-oxidising) and rich (net-reducing) conditions. When calcined in air, alloy Pd–Pt nanoparticles are present only on catalysts subjected to elevated temperature (800 °C) whereas calcination at lower temperature (500 °C) leads to segregated Pt and Pd nanoparticles on the support. Here, we show that the alloy Pd–Pt nanoparticles undergo reversible changes in surface structure and composition during transient methane oxidation exposing a PdO surface during lean conditions and a metallic Pd–Pt surface (Pd enriched) under rich conditions. Alloyed particles seem more active for methane oxidation than their monometallic counterparts and, furthermore, an increased activity for methane oxidation is clearly observed under lean conditions when PdO has developed on the surface, analogous to monometallic Pd catalysts. Upon introducing rich conditions, partial oxidation of methane dominates over total oxidation forming adsorbed carbonyls on the noble metal particles. The carbonyl spectra for the three samples show clear differences originating from different surfaces exposed by alloyed vs. non-alloyed particles. The kinetics of the noble metal oxidation and reduction processes as well as carbonyl formation during transient methane oxidation are discussed.
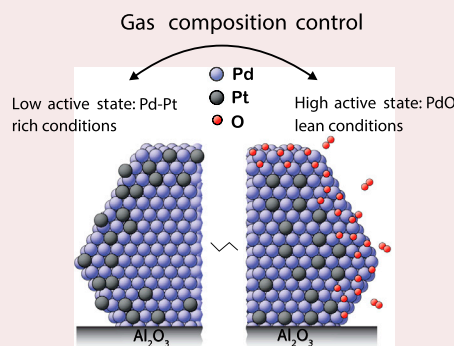
Introduction

Hydrocarbon emissions from natural gas engines consist mostly of unburned methane. As methane is a strong greenhouse gas, it is of vital importance to remove it from the exhausts. Palladium-based catalysts have been extensively explored for the complete combustion of CH_4 thanks to facile methane dissociation, a step that is often considered to be rate-determining. Among those catalysts, the bimetallic Pd–Pt system has attracted interest [1–4]. Recent studies report that supported Pd–Pt catalysts exhibit higher sulfur tolerance and long-term stability than supported Pd alone and may show improved activity for methane oxidation with time [1,4–9]. Also, Pd–Pt catalysts are less prone to sintering in oxidative environments compared to supported Pt only [10].

For monometallic Pd catalysts, significant amount of work has been focused on understanding the active phase of Pd during methane oxidation. Previous results show that a particular facet of bulk palladium oxide, PdO(101), has a uniquely high activity for the complete oxidation of methane at low temperatures [11,12].

The reason being that the PdO(101) surface expose under-coordinated sites that facilitate the dissociation of methane. One may envisage that such sites, or similarly under-coordinated sites, can exist on supported Pd particles under oxidising conditions, explaining the observed high activity for Pd-based catalysts. On the contrary, for Pt catalysts, the formation of platinum oxides is detrimental for methane oxidation. Instead, the metallic surface is active. Transient operation, however, of the feed gas stoichiometry can be used to promote methane oxidation over supported Pt catalysts by minimising the detrimental effect of oxygen [13,14]. In fact, in comparison with metallic Pt prevailing under net-reducing conditions, transient operation may induce an even more (non-stable) active state that is rich in highly reactive oxygen species [15,16]. Hence, when supported on alumina, Pd is the most active metal for lean operation conditions whereas Pt is more efficient when rich conditions prevail [17]. For bimetallic Pd–Pt catalysts, however, little is known about the oxidation behavior of the bimetallic phase and its relation to the catalytic activity for methane oxidation.

Automotive catalysts frequently operate in dynamic environments, alternating between net-oxidising (lean) and net-reducing (rich) conditions, such that the surface composition and structure of the catalyst continuously change. For example, such treatments may induce significant reconstructions in the surface structure of bimetallic catalysts [18–21]. This can have dramatic effects on the overall performance of the catalyst as the catalytic properties change correspondingly. In our recent publication [22] we have studied the influence of catalyst calcination conditions on the oxidation and reduction behavior of bimetallic Pd–Pt catalyst. It is shown that bimetallic Pd–Pt nanoparticles are formed after calcination at high temperature, 800 °C, both in dry and wet air. The bimetallic nanoparticles expose a Pd–Pt metallic surface enriched in Pd under reducing conditions, while under oxidising conditions a PdO phase dominates the surface. PdO is present both in form of crystals at the surface of the Pd–Pt particles and as isolated PdO crystals on the support oxide. However, for the sample calcined at 500 °C, no alloy formation is observed, but individual monometallic Pd or Pt nanoparticles that are oxidised to PdO and PtO_x under oxidising conditions.

The present study addresses low-temperature oxidation of methane during lean-rich cycling over Pd–Pt/Al_2O_3 catalysts that have been calcined at different temperatures and atmospheres. In particular we have employed *operando* Fourier transform infrared spectroscopy (FTIR) and *in situ* X-ray absorption spectroscopy (XAS) to follow the evolution of surface species and changes in chemical state of the Pd–Pt phase, respectively, during lean-rich cycling. The composition of the effluent stream was monitored by mass spectrometry (MS). The results show that the changes in activity for methane oxidation over bimetallic Pd–Pt catalysts correlate to changes in white line intensity of the Pd K edge in X-ray absorption spectra. Further, the changes in methane conversion observed when dynamically changing feed gas stoichiometry are strongly connected to oxidation and reduction of the active Pd phase. An increased activity is observed when PdO forms on the surface of the bimetallic Pd–Pt nanoparticle samples. The surface speciation reveals that carbonyls adsorbed on the noble metals are formed during rich conditions and a clear difference is observed in the carbonyl infrared spectra for the alloyed compared to the non-alloyed particle samples.

Experimental section

Catalyst preparation

Model catalysts with 2.0 wt.% Pd and 0.4 wt.% Pt supported on γ-Al_2O_3 were prepared by incipient wetness impregnation followed by calcination in either air at 500 °C for 2 h, in air 800 °C for 10 h or in air with addition of 10% water at 800 °C for 10 h. The different samples are summarised in Table 1. For simplicity, the samples will hereafter be referred to by their sample ID. The as prepared catalysts have been characterised *ex situ* by X-ray diffraction and transmission electron microscopy (TEM) as described in more detail in our recent publication [22]. *Operando* FTIR and MS, and *in situ* XAS were employed to study the methane oxidation over the bimetallic Pd–Pt catalysts as described below.

In situ XAS measurements

The *in situ* XAS measurements of the platinum phase were performed at beamline I811 at MAX IV Laboratory, Lund, Sweden [23,24]. The Pt L_{III} edge at 11,564 eV was measured in fluorescence mode (45° geometry). A Pt foil was used for energy calibration. The XAS measurements included both the X-ray absorption near edge structure (XANES) and the extended X-ray absorption fine structure (EXAFS) regions. Fourier transformation of the k^2-weighted EXAFS data to the R space was done between $k = 3$ and $k = 14 \, Å^{-1}$ for the Pt L_{III} edge. Steady-state methane oxidation experiments feeding 0.1% CH_4 and 1.4% O_2 (for 30 min) at a sample temperature of 360 °C to a specially designed reaction cell [25] were performed. Prior to the methane oxidation experiments the samples were reduced in a flow of hydrogen (5% H_2) at 360 °C.

The time-resolved *in situ* XAS measurements of the palladium phase were performed at the energy-dispersive (ED) beamline ID24 at the European Synchrotron Radiation Facility (ESRF) in Grenoble, France [26]. The Pd K edge at 24,350 eV was measured in

Table 1. Nomenclature, noble metal content, calcination conditions and (rough average) particle size for the Pd–Pt catalysts samples. Particle sizes were estimated from TEM analysis of the as-prepared samples.

Sample ID	Noble metal content		Calcination conditions	Particle size		
	Pd (wt.%)	Pt (wt.%)		Pd (nm)	Pt (nm)	PdPt (nm)
Pd–Pt F500	2.0	0.4	Air at 500 °C for 2 h	5–20	1–10	–
Pd–Pt F800	2.0	0.4	Air at 800 °C for 10 h	5–10	–	50–100
Pd–Pt L800	2.0	0.4	Air with 10% H_2O at 800 °C for 10 h	5–10	–	50–100

transmission mode using synchronous MS, see below. Energy calibration was performed using a Pd metal foil. The measurements were performed using a Si[311] polychromator in Bragg configuration and a FreLoN detector. The experimental set-up included a specially designed reaction cell developed at ID 24, which has a small reactor volume in which a sample cup with a diameter 5 mm and a depth 2.5 mm loaded with about 40 mg of catalyst powder is positioned. The gas composition is controlled by mass flow controllers (Bronkhorst) and introduced to the cell via air-actuated high-speed gas valves (Valco, VICI). All in all facilitating rapid gas composition changes over the catalyst sample. Details of the experimental setup and analysis have been described previously [22,27].

At ESRF, methane oxidation measurements were performed at 360 °C with 3 min length pulses of 1.5% O_2 in an otherwise constant flow of 0.1% CH_4. The pulses were repeated eight times to give a total duration of the experiment of 48 min. The introduction of the first O_2 pulse triggered the recording of the XAS spectra. He was used as carrier gas, and the total gas flow was kept constant at 75 ml/min.

Operando FTIR

The *operando* FTIR measurements were performed in diffusive reflectance (DRIFT) mode with a BRUKER Vertex 70 spectrometer equipped with a high-temperature stainless steel reaction cell (Harrick Praying Mantis^{TM} High Temperature Reaction Chamber) with KBr windows and a nitrogen-cooled MCT detector. The reaction cell contains a sample cup with a diameter of 6 mm and a depth of 3 mm. The wavenumber region between 790 and 3800 cm^{-1} was measured with a spectral resolution of 4 cm^{-1}. The temperature of the sample holder was measured by a thermocouple (type k) and controlled by a PID regulator (Eurotherm). Feed gases were introduced into the reaction cell via individual mass flow controllers, providing a total flow of 100 ml/min in all experiments. Moreover, the O_2 feed was introduced via a high-speed gas valve (Valco, VICI) in order to provide precise transients. Prior to each experiment the samples were pre-treated at 500 °C with 2% O_2 in Ar for 10 min and 1% H_2 in Ar for 10 min and then a background spectrum was collected after the sample has been cooled to 360 °C in a Ar flow. The catalytic performance of the catalysts for methane

oxidation was measured at 360 °C with 3 min length pulses of 1.5% O_2 in an otherwise constant flow of 0.1% CH_4 at a constant 100 ml/min total flow. The pulses were repeated 12 times and the spectra were recorded every 4.3 s. After the last $CH_4 + O_2$ pulse, 0.05% CO was introduced to the reaction cell for 10 min, also at a constant 100 ml/min total flow. The product stream was continuously analysed by MS (Hidden Analytical, HPS-20 QIC) following the m/e ratios 2 (H_2), 15, 16 (CH_4), 18 (H_2O), 28 (CO), 40 (Ar) and 44 (CO_2).

Results and discussion

The results from the spectroscopic and kinetic measurements of methane oxidation over the three Pd–Pt/Al_2O_3 catalysts during periodic variation of the feed gas composition between 1.5% O_2 + 0.1% CH_4 (net-oxidising or lean conditions) and 0.1% CH_4 (net-reducing or rich conditions) at a sample temperature of 360 °C are shown in Figure 1. The figure displays data for the fifth to seventh cycle in the lean-rich cycle sequence, i.e, pulses for which repeatable responses are achieved, where periods with lean conditions are shaded pale red. Omitting the first cycles is a generally established approach in this type of pulse-response experiment, as during an initial period, the system under study usually undergoes some dynamical changes for which the measured responses are not repeatable. The top panels show the color-coded intensities (red corresponds to high intensity, blue to low intensity) of the DRIFT spectra in the wavenumber region 1200–3800 cm^{-1} vs. time, while the middle panels show the white line intensity of the Pd K edge measured with ED XAS. Finally the MS kinetic data, i.e. outlet concentrations of CH_4, CO_2, O_2 and H_2, are shown in the bottom panels. The DRIFTS/MS data have been recorded simultaneously in a true *operando* approach in our home laboratory, while the *in situ* XAS data have been collected at the synchrotron. For this reason slightly different reaction cells were used, as described above, which potentially may cause some discrepancies due to, in the first place, different dead volumes. Fortunately, however, this has no severe implications on the interpretations of the results, for which the trends can be well compared and correlated, especially during the lean periods, as will be discussed below.

During the cycling experiment the evolution of IR absorption bands corresponding to adsorbed carbonyls,
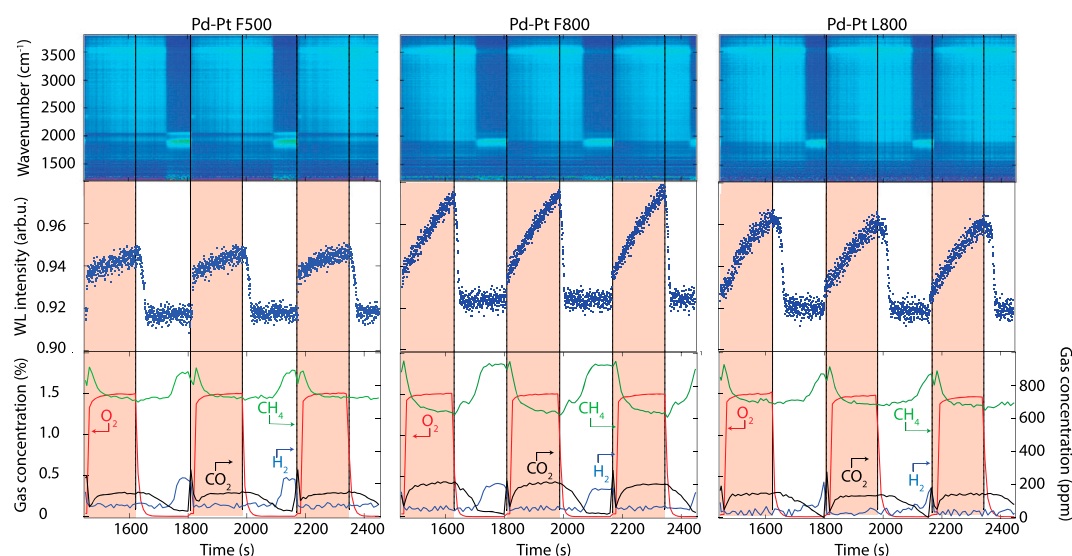
Figure 1. Transient oxidation of 0.1% CH_4 over the Pd–Pt/Al_2O_3 F500 (left panels), Pd–Pt/Al_2O_3 F800 (middle panels) and Pd–Pt/Al_2O_3 L800 (right panels) catalysts during periodic variation of the feed gas composition between lean (0.1% CH_4 and 1.5% O_2, pale red marked areas) and rich (0.1% CH_4) periods for 180 s at 360 °C. The top panels show the color coded intensities (blue corresponds to low intensity, red to high intensity) of the IR absorption bands in the region 1200–3800 cm^{-1} vs. time recorded during the lean-rich cycling experiment. The middle panels show the evolution of the XAS white line intensity (WLI) at 24,372 eV. The bottom panels show the outlet concentration of O_2 (red), CO_2 (black), CH_4 (green) and H_2 (blue) measured by MS.

i.e. CO adsorbed on the noble metal particles, are observed in the region 1800–2000cm^{-1} for all samples during the second half of the rich periods. For the F500 sample, the formation of CO gives rise to both linearly bound carbonyls (IR bands at higher wavenumbers) and bridge-bonded carbonyls (IR bands at lower wavenumbers), which rapidly are oxidised and thus disappear from the spectra directly after the switch to the lean phase. For the F800 sample, the carbonyl bands form earlier compared to the F500 sample while for the L800 sample a delay is observed. For both the F800 and L800 samples, mostly the carbonyl band at lower wavenumbers is visible, reflecting that bridge-bonded CO is the dominating carbonyl species. Upon introduction of oxygen, the adsorbed carbonyl species vanish abruptly due to the fast CO oxidation reaction as for the F500 sample. The evolution of linear carbonyls (integration of IR bands in the region 2000–2100 cm^{-1}) and bridged carbonyls (integration of IR bands between 1730 and 2000 cm^{-1}) on the metal (Pd, Pt or PdPt) vs. time are shown in Figure S1 (Supporting Information), together with the CO outlet concentration measured by MS. A clear difference between the linear vs. bridged carbonyl species for the F800 and L800 samples compared to F500 sample is seen. This will be discussed in more detail below.

The white line intensity of the Pd K edge has been used to follow the change in the oxidation state of Pd as previously reported [27], and the results, summarised in the middle panel of Figure 1, show that the changes in activity for CH_4 oxidation can be connected to changes in white line intensity in the X-ray absorption spectra.

There is an increase in the white line intensity during the lean periods for all samples and the spectra resemble the PdO spectrum, suggesting the formation of PdO, while there is a fast decrease of the white line intensity at the switch to rich periods suggesting a reduction to a metallic Pd state, in agreement to our previous findings on the oxidation/reduction behavior of Pd–Pt catalysts [22]. Therefore, we expect a restructuring of the surface of the bimetallic nanoparticles to occur during the dynamic methane oxidation experiments. A clear difference in the oxidation behavior of the F500, F800 and L800 samples can be seen, where the latter two show a continuous increase in the oxidation state of Pd during the lean periods. This suggests that the alloyed nanoparticles obey a different oxidation kinetics compared to the monometallic nanoparticles during methane oxidation, which may be due to alloying, that can affect the oxide formation, but also different particle size distribution and/or shape. When switching to rich conditions the samples are reduced following a process with considerably faster kinetics compared to the oxidation process. The reduction of the L800 samples is fastest followed by the F500 and L800 samples.

Since our previous results on the oxidation behavior of Pd–Pt catalysts reveal oxidation of Pt for the F500 sample, a similar experiment has been performed by measuring the Pt L_{III} edge during methane oxidation. Figure 2 displays the Pt L_{III} edge XANES (a) and EX-AFS (b) spectra recorded *in situ* during oxidation of 0.1% CH_4 with 1.4% O_2 at 360 °C. The XANES spectrum for the F500 sample shows an increase in the white line intensity indicating that Pt is in an oxidised
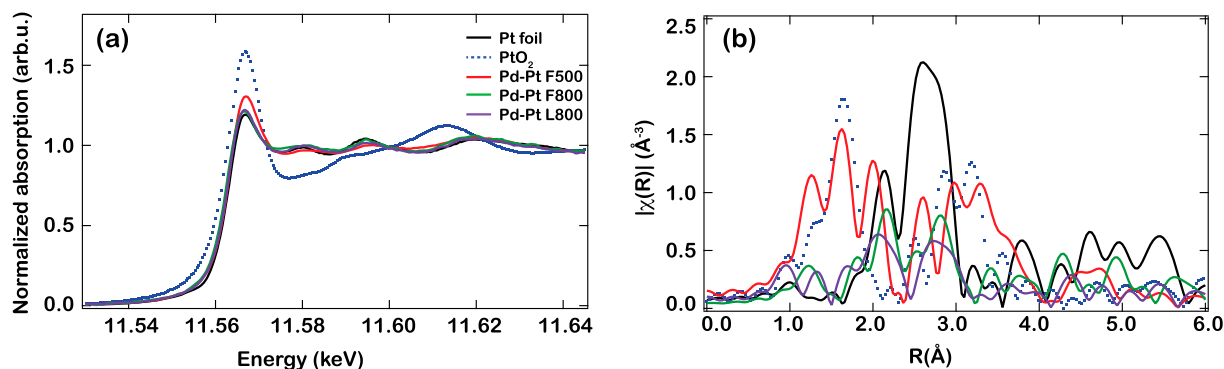
Figure 2. Pt L$_{III}$ edge *in situ* XAS spectra for the Pd–Pt/Al$_2$O$_3$ catalysts during methane oxidation (0.1% CH$_4$ and 1.4% O$_2$) at 360 °C. Pt foil and PtO$_2$ are included as references. (a) XANES spectra and (b) Magnitude of Fourier transform EXAFS spectra (k-weight = 2).

state, in contrast to the spectra for the F800 and L800 samples that are similar to the spectrum for Pt foil. The associated Fourier transforms are shown in Figure 2(b), where R represents the radial distance from the adsorbing atom. The spectra for the F800 and L800 samples feature a double peak at about 2.2 and 2.7 Å similar to the Pt foil reference spectrum, which has been attributed to Pt–M bond (M = Pt or Pd). For the F500 sample some peaks are observed at significantly shorter distance, suggesting a Pt–O bond in agreement to our previous results on the oxidation of Pd–Pt catalysts [22]. Thus, the XAS results suggest that during lean methane oxidation conditions both Pd and Pt are oxidised for the F500 sample, while only Pd is oxidised for the F800 and L800 samples.

The concentrations in the effluent stream for all samples are qualitatively similar to our previous results on lean methane oxidation over Pd/Al$_2$O$_3$ [27]. During lean-rich cycling, temporary high activity for methane oxidation is seen at the switches to the lean periods as has been reported previously for both Pd and Pt supported on alumina [13]. This is due to a transition from a reduced to an oxidised surface that involves a passage of a surface composition that is beneficial for the catalytic activity. Additionally, the introduction of an oxygen pulse initially results in a temporary over-production of CO$_2$, which is due to the oxidation of accumulated carbonaceous species such as CH$_x$ and CO on the metal surface, as for the latter indicated by the rapid decrease in adsorbed carbonyls. After passing this transient regime, the activity decreases for a short period of time. The lower white line intensity during this state suggests that the Pd surface is being either covered with chemisorbed O atoms or a surface oxide that hinders methane oxidation as previously reported [12]. Upon further oxygen exposure, the catalysts regain activity, increasing methane conversion, which correlates with the increase in white line intensity of Pd, i.e. bulk oxidation of the Pd particles becoming more active. Thereafter a steady state conversion is reached for the remaining of the lean period. At the switches to rich

conditions, the CO$_2$ formation declines slowly towards a low stationary level for the F500 sample while for the F800 and L800 samples the formation CO$_2$ rather drops within about one and a half and three minutes, respectively. For all samples the slipped methane starts to increase during the second half of the rich period. The increase appears earlier for the F800 sample compared to the F500 and L800 samples. Further, the F800 sample shows a faster transition between total methane oxidation to partial oxidation as illustrated by an increase in H$_2$ formation as well as adsorbed carbonyls, which can be due to smaller particle sizes. The decrease of the white line intensity appears faster than the decline in methane conversion as well as evolution of surface carbonyls for all samples. Although this difference may be attributed to differences in the experimental set-up between the two experiments (DRIFTS/MS vs. XAS) it may well be a real effect. For example, it is known that relatively large amounts of oxygen can be incorporated into the Pd structure, especially for small Pd particles [28]. Depending on the methane concentration at the surface of the particles, this may lead to a prolonged process for complete reduction of all particles such that the DRIFTS/MS measurements becomes more influenced than the XAS measurement due to higher surface sensitivity of DRIFTS and the catalytic processes as compared to the XAS.

Comparing the different Pd–Pt samples, it is clear that the activity for the ones containing alloyed nanoparticles (F800 and L800) is superior to the sample containing monometallic nanoparticles (F500), in agreement with previous reports [1,5,8]. This may be due to the increased amount of PdO for the alloyed nanoparticles samples, which is also indicated by the increased white line intensity in Figure 1. However, a difference in activity between the F800 and L800 samples can also be observed. The understanding of this is presently not clear and further measurements are needed to elucidate the underlying mechanism. A possible explanation may be that the smaller particles for the F800 sample result in higher amount of PdO
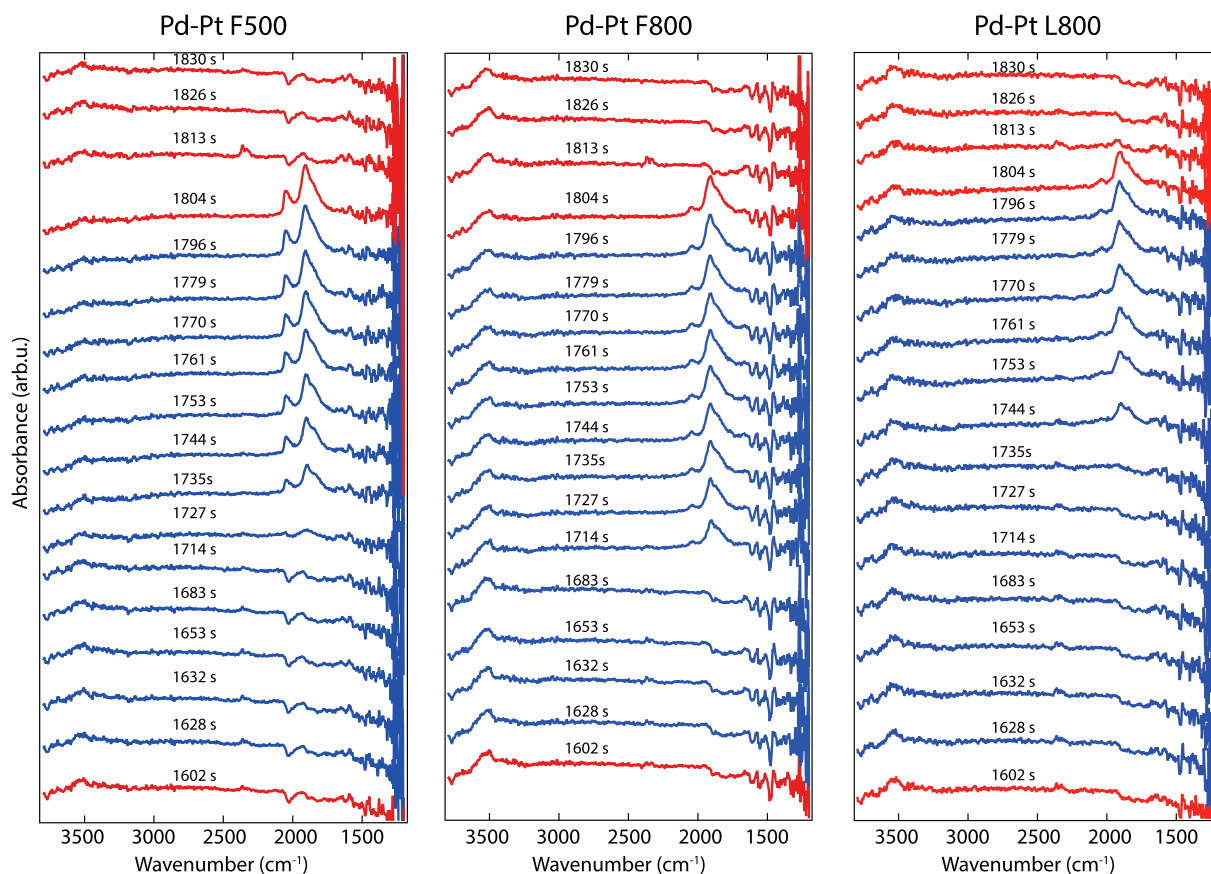
Figure 3. Evolution of IR absorption bands in the wavenumber region 1200–3800 cm^{-1} for the Pd–Pt/Al_2O_3 F500 (left panel), Pd–Pt/Al_2O_3 F800 (middle panel) and Pd–Pt/Al_2O_3 L800 (right panel) catalysts exposed to CH_4 and O_2 while changing the feed gas composition from 0.1% CH_4 + 1.5%O_2 (red, below 1620 s) and 0.1% CH_4 (blue, between 1620 and 1800 s) and back to 0.1% CH_4 + 1.5%O_2 (red, above 1800 s) at 360 °C. The insert numbers indicate the time (s) in the dynamic experiment where the spectra were recorded.
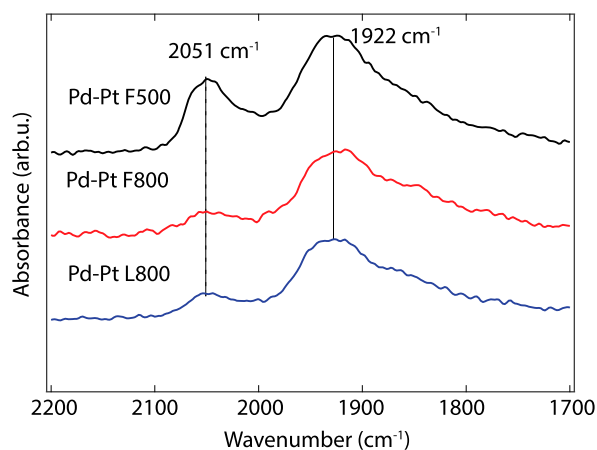
Figure 4. Evolution of IR absorption bands in the wavenumber region 1700–2200 cm^{-1} for the Pd–Pt/Al_2O_3 F500 (black), Pd–Pt/Al_2O_3 F800 (red) and Pd–Pt/Al_2O_3 L800 (blue) catalysts exposed to 0.05% CO for 10 min after methane oxidation reaction at 360 °C.

being formed during lean methane oxidation (also illustrated by the increased white line intensity), which is beneficial for the methane oxidation reaction. This might explain the faster reduction of the F800 sample

compared to the L800 sample during the rich periods. Unfortunately, enough particle size distribution data are presently not available and thus only (rough average) particle size values are given in Table 1. Overall, the results show an increased activity for methane oxidation under lean conditions when PdO forms on the surface of the bimetallic Pd–Pt catalysts, consistent with previous reports on methane oxidation over Pd [11,12,29,30].

To better understand the changes in surface species composition during periodic operation, a number of DRIFT spectra are shown in Figure 3 during a lean-rich cycle (from 1600 to 1830 s) for the F500 (left), F800 (middle) and L800 (right panels) samples at 360 °C when the feed of CH_4 + O_2 (below 1620 s) is changed to only CH_4 flow (1620–1800 s) and back to CH_4 + O_2 (above 1800 s). The spectra reveal noticeable changes of the position and intensity of the IR bands during the cycle. The insert numbers indicate the time (in seconds) in the dynamic experiment from where the spectra were extracted. The first spectra show the absorption bands just before the introduction of the oxygen pulse. The major changes in the IR spectra take place during the rich phase, where carbonyl bands within the

$1800-2100 \, \text{cm}^{-1}$ region start to appear. For all samples, the formation of CO species adsorbed on the metallic surface (the wavenumber region between 1800 and $2100 \, \text{cm}^{-1}$) are observed during the second half of rich period when the outlet concentrations in Figure 1 (bottom panels) show a fast decrease of the methane oxidation activity. In addition, the formation of some carbonate species on alumina (the wavenumber region between 1200 and $1600 \, \text{cm}^{-1}$) is observed during nearly the entire experiment. The intensity of these species is low compared to the carbonyl species and also disturbed by the emitting alumina support in the low wavenumber region at these conditions. Further, a broad band centered around $3575 \, \text{cm}^{-1}$ is observed during both lean and rich periods, with higher intensity for the F800 and L800 samples compared to the F500 sample, together with some weak negative peaks above $3800 \, \text{cm}^{-1}$. The band at around $3575 \, \text{cm}^{-1}$ is assigned to associated hydroxyl groups, mutually interacting by hydrogen bonding, perturbing the surface hydroxyl groups leading to negative peaks in the higher wavenumber region.

Returning to the adsorbed CO species, both the linearly bound and bridge-bonded carbonyls are observed for the F500 sample (linear at $2050 \, \text{cm}^{-1}$ and bridged at $1920 \, \text{cm}^{-1}$). In contrast, the intensity of the linearly adsorbed CO is lower for the F800 and L800 samples such that bridge-bonded CO becomes the domination contribution. Alloying might affect the lattice parameters and electronic properties of Pd and Pt, which in turn could affect the adsorption properties of the noble metal particles, explaining the observed differences between the samples. No noticeable shifts are observed for the carbonyl bands during the rich period for any sample. It is interesting, though, to note that the carbonyl species appear with different time lag for the three samples. The F800 sample shows the first carbonyl band at about 90 s after the oxygen has been switched off, followed by the F500 sample (110 s) and L800 sample (120 s). The time at which carbonyls appear signifies the transition from total methane oxidation on oxidised noble metal surfaces to partial methane oxidation over reduced noble metal particles (as CO adsorbs preferentially on reduced sites) and thus the various time lags reflect different reduction kinetics for the noble metal particles. This may be due to that smaller particles are reduced faster than larger ones but also due to the alloying, which is likely to affect the adsorption properties. About 10 s after the introduction of O_2, there are some changes in the DRIFT spectra: the carbonyl bands disappear and gas phase CO_2 peaks appear (centered at $2350 \, \text{cm}^{-1}$), which is likely the result of the oxidation of CH_x and CO species accumulated on the surface during the rich period.

Summarising the *operando* DRIFTS/MS measurements, we note as a main result that when partial methane oxidation occurs at the expense of total oxidation of methane the formation of a variety of carbonyl species adsorbed on the noble metal nanoparticles occurs. Interesting differences between the different samples can be discerned: the presence of both linearly bound and bridge-bonded CO species is observed for the F500 sample, while bridge-bonded CO species dominate for the F800 and L800 samples. This suggests that the surface composition is different for the different samples, i.e. samples calcined at 800 °C vs. the sample calcined at 500 °C. It is known that there are some surface reconstructions of the bimetallic Pd–Pt nanoparticles when exposed to oxidising/reducing conditions. The F500 sample, containing non-alloyed nanoparticles, exposes similar amounts of Pd and Pt at the surface under reduction conditions, while the F800 and L800 samples expose both Pd and Pt, although enriched in Pd, at their surfaces [22]. It is likely that this may cause the observed differences in the carbonyl spectra for the alloyed (F800 and L800) vs. the non-alloyed (F500) samples.

Isothermal CO exposure measurements

As the carbonyl spectra formed during rich periods in the transient methane oxidation experiments are significantly different for the alloyed vs. non-alloyed samples, CO was used as a probe molecule to characterise the surface of the bimetallic Pd–Pt catalysts in more detail. Figure 4 shows the DRIFT spectra for isothermal CO exposure subsequently after methane and oxygen have been removed from the feed at the end of the methane oxidation experiments performed at 360 °C. Selected spectra during the course of the CO exposure measurements for 10 min are presented in Figure S2 (Supporting Information).

Upon switching off the oxygen supply, CO starts to accumulate on the metal nanoparticles, which become reduced. It is interesting to note that no clear shift in the carbonyl band is observed as was also the case for the cycled methane oxidation experiments discussed above. This reflects that CO adsorbs on chemically stable (reduced) sites on Pd, Pt and Pd–Pt or, expressed differently, at these temperatures CO cannot adsorb onto the noble metal particles unless these are significantly reduced. The coverage of CO on the noble metal increases on all samples, at about 2 min after the CO feed has been switched on, similar to CH_4 exposure data presented in Figure 3 above (rich periods). In the case of the F500 sample, two strong absorption bands at 2051 and $1922 \, \text{cm}^{-1}$ develop, i.e. the linearly bound and bridge-bonded CO bands. For the F800 and L800 samples, the intensity of the linearly adsorbed CO has decreased, and an increase in the bridge-bonded CO is observed at around $1922 \, \text{cm}^{-1}$. In addition, a band corresponding to bridge-bonded CO can be observed

at 1850 cm^{-1}. Even though it is not clear whether these bands could be related to Pt sites, Pd sites or Pd–Pt sites, the observed differences indicate that CO adsorbs on different sites for the F500 sample vs. the F800 and L800 catalysts.

In an earlier report, Lapisardi et al. [8] have compared the IR spectra of CO adsorbed on Al$_2$O$_3$-supported Pd, Pt and Pd–Pt catalysts. The authors show that CO adsorbs mainly linearly on atop surface sites of Pt particles of Pt/Al$_2$O$_3$, giving rise to a single intense CO band around 2070 cm^{-1}, while CO was found to adsorb both linearly and in bridged form on Pd surface sites of Pd/Al$_2$O$_3$, giving rise to a weak absorption band around 2070 cm^{-1} and multiple broad absorption bands below 2000 cm^{-1}, as also reported by Garbowski et al. [31]. This is also in agreement with our previous report on CO adsorption on clean and oxidized Pd surfaces, which shows that CO adsorbs on a c(4×2) configuration on both hcp and bridge sites on the Pd(111) surface [32]. When CO was adsorbed on bimetallic Pd–Pt catalysts (high Pd:Pt molar ratio, as in the present case), a decrease and a broadening of the band mainly characteristic of CO adsorbed on Pt surface has been noted (band at 2070 cm^{-1}) together with a broad band between 1800 and 2000 cm^{-1} [8]. Further, the temperature may induce a shift in the IR absorption bands, which for CO adsorbed on Pt has been reported to be 2051 cm^{-1} at 360 °C, and 2069 cm^{-1} at 280 °C [33]. Based on these observations, we assign the CO absorption band observed in our measurements at 2051 cm^{-1} to linearly adsorbed CO on mostly Pt sites, while the band at lower wavenumbers is assigned to CO bridge-bonded to mostly Pd. Thus, the CO adsorption measurements (as well as the partial methane oxidation results) suggest that CO adsorbs on both Pd and Pt sites on the F500 sample, while it adsorbs mostly on the Pd sites for the F800 and L800 samples. This indicates that both Pd and Pt are exposed at the surface of the F500 sample, while mostly Pd is present at the surface of the F800 and L800 samples, in good agreement with our recent publication and supporting the results of alloy formation for the F800 and L800 samples [22].

Conclusions

This work presents a study of transient effects in the methane oxidation reaction over a series of bimetallic Pd–Pt catalysts supported on alumina and calcined at different temperatures and conditions. A good understanding of how the catalytic activity for methane oxidation and formed surface species depend on the feed stoichiometry and chemical state and structure of the Pd–Pt nanoparticles is demonstrated using *operando* DRIFTS and *in situ* XAS techniques. It is shown that changes in methane conversion observed when dynamically changing feed conditions are directly connected to oxidation and reduction of the active Pd phase. An increased activity is observed when PdO forms on the surface of the bimetallic Pd–Pt nanoparticles. *In situ* DRIFTS experiments show that adsorbed carbonyl species are formed during rich conditions over all studied catalysts, suggesting a similar reaction mechanism as previously observed for Pd catalysts. For the samples initially calcined at 800 °C, clear differences in the carbonyl spectra are observed as compared to the sample calcined at lower temperature, which indicate an interaction between Pd and Pt in these samples. Further, the measurements suggest that the F500 sample expose both Pd and Pt during reaction conditions, while mostly Pd is exposed for the samples calcined at 800 °C, which is oxidised to PdO under lean conditions. The results support previous reports on the most active phase of Pd during lean methane oxidation conditions being PdO and extends this conclusion to bimetallic Pd–Pt catalysts.

ORCID

Natalia M. Martin http://orcid.org/0000-0002-6881-4989
Johan Nilsson http://orcid.org/0000-0001-5056-6289
Magnus Skoglundh http://orcid.org/0000-0001-7946-7137
Emma C. Adams http://orcid.org/0000-0003-4341-3713
Per-Anders Carlsson http://orcid.org/0000-0001-6318-7966

References

[1] Persson K, Eriksson A, Jansson K, et al. Influence of molar ratio on Pd-Pt catalysts for methane combustion. J Catal. 2006;243:14–24.
[2] Persson K, Jansson K, Järås S. Characterisation and microstructure of Pd and bimetallic Pd-Pt catalysts during methane oxidation. J Catal. 2007;254:401–414.

[3] Ersson A, Kusar H, Carroni R, et al. Catalytic combustion of methane over bimetallic catalysts a comparison between a novel annular reactor and a high-pressure reactor. Catal Today. 2003;83:265–277.

[4] Ozawa Y, Tochihara Y, Watanabe A, et al. Stabilizing effect of Nd_2O_3, La_2O_3 and ZrO_2, on $Pt \cdot PdO/Al_2O_3$ during catalytic combustion of methane. Appl Catal A: General. 2004;258:261–267.

[5] Narui K, Yata H, Furata K, et al. Effects of addition of Pt to $PdO=Al_2O_3$ catalyst on catalytic activity for methane combustion and TEM observationsof supported particles. Appl Catal A: General. 1999;179:165–173.

[6] Ishihara T. Effects of Additives on the Activity of Palladium Catalysts for Methane Combustion. Chem Lett. 1993;22:407–410.

[7] Yamamoto H, Uchida H. Pt and Pd Supported on Alumina in Lean-burn Natural-gasEngine Exhaust. Catal Today. 1998;45:147–151.

[8] Lapisardi G, Urfels L, Gelin P, et al. Superior catalytic behaviour of Pt-doped Pd catalysts in the complete oxidation of methane at low temperature. CatalToday. 2006;117:564–568.

[9] Strobel R, Grunwaldt J-D, Camenzind A, et al. Flame-made alumina supported Pd–Pt nanoparticles: structural properties and catalytic behavior in methane combustion. Catal Lett. 2005;104:9–16.

[10] Chen M, Schmidt LD. Morphology and composition of PtPd alloy crystallites on SiO_2 in reactive atmospheres. J Catal. 1979;56:198–218.

[11] Hellman A, et al. The Active Phase of Palladium during Methane Oxidation. J Phys Chem Lett. 2012;3:678–682.

[12] Martin NM, et al. Intrinsic Ligand Effect Governing the Catalytic Activity of Pd Oxide Thin Films. ACS Catal. 2014;4:3330–3334.

[13] Carlsson PA, Fridell E, Skoglundh M. Methane oxidation over Pt/Al_2O_3 and Pd/Al_2O_3 catalysts under transient conditions. Catal Lett. 2007;115:1–7.

[14] Carlsson P-A, Nordström M, Skoglundh M. Virtual control for high conversion of methane over supported Pt. Top Catal. 2009;52:1962–1966.

[15] Becker E, Carlsson P-A, Grönbeck H, et al. Methane oxidation over alumina supported platinum investigated by time-resolved *in situ* XANES spectroscopy. J Catal. 2007;252:11–17.

[16] Becker E, Carlsson P-A, Kylhammar L, et al. In situ spectroscopic investigation of low-temperature oxidation of methane over alumina-supported platinum during periodic operation. J Phys Chem C. 2011;115:944–951.

[17] Burch R, Loader PK, Urbano FJ. Some aspects of hydrocarbon activation on platinum group metal combustion catalysts. Catal Today. 1996;27:243–248.

[18] Somorjai GA. Introduction to surface chemistry and catalysis. New York (NY): Wiley-VCH; 1994.

[19] Johnson WC, Blakely JM, editors. Interfacial segregation. Metals Park (OH): American Society for Metals; 1979.

[20] Chelikowsky JR. Predictions for surface segregation in intermetallic alloys. Surf Sci. 1984;139:L197–L203.

[21] du Plessis J. Surface segregation; Solid State Phenomena. Vol. 11, Vaduz, Liechtenstein: Sci-Tech Publications; 1990.

[22] Martin NM, Nilsson J, Skoglundh M, et al. Characterization of surface structure and oxidation/reduction behavior of Pd-Pt/Al_2O_3 model catalysts. J Phys Chem C. 2016;120:28009–28020.

[23] Grehk TM, Nilsson PO. The design of the material science beamline, I811, at MAX II. Nucl Instr Meth Phys Res A. 2001;635:467–468.

[24] Carlson S, Clausen M, Gridneva L, et al. XAFS experiments at beamline I811, MAX-lab synchrotron source, Sweden. J Synchrotron Rad. 2006;13:359–364.

[25] Zhang C, Gustafson J, Merte LR, et al. An in situ sample environment reaction cell for spatially resolved X-ray absorption spectroscopy studies of powders and small structured reactors. Rev Sci Instr. 2015;86:033112-1–033112-7.

[26] Pascarelli S, et al. J Synchrotron Rad. 2016;23:353–368.

[27] Nilsson J, Carlsson P-A, Fouladvand S, et al. Chemistry of supported palladium nanoparticles during methane oxidation. ACS Catal. 2015;5:2481–2489.

[28] Schalow T, Brandt B, Starr DE, et al. Size-dependent oxidation mechanism of supported Pd nanoparticles. Angew Chem Int Ed. 2006;45:3693–3697.

[29] Weaver JF, Hakanogl C, Hawkins JM, et al. Molecular adsorption of small alkanes on a PdO(101) thin film: Evidence of σ -complex formation. J Chem Phys B. 2010;2:024709.

[30] Weaver JF, Hinojosa JA, Hakanoglu C, et al. Precursor-mediated dissociation of n-butane on a PdO (101) thin film. Catal Today. 2011;160:213–227.

[31] Garbowski E, Feumi-Jantou C, Mouaddib N, et al. Catalytic combustion of methane over palladium supported on alumina catalysts: Evidence for reconstruction of particles. Appl Catal A. 1994;109:277–291.

[32] Martin NM, van den Bossche M, Grönbeck H, et al. CO adsorption on clean and oxidised Pd(111). J Phys Chem C. 2014;118:1118–1128.

[33] Becker E, Carlsson P-A, Kylhammar L, et al. In situ spectroscopic investigation of low-temperature oxidation of methane over alumina-supported platinum during periodic operation. J Phys Chem C. 2011;115:944–951.